

## Cellular interactions implicated in the mechanism of photoreceptor degeneration in transgenic mice expressing a mutant rhodopsin gene

PATTI C. HUANG\*, ALICIA E. GAITAN\*, YING HAO\*, ROBERT M. PETERS†, AND FULTON WONG\*‡§

\*Department of Ophthalmology, and †Department of Neurobiology, Duke University School of Medicine, Durham, NC 27710; and ‡Department of Animal Science, North Carolina State University, Raleigh, NC 27695

Communicated by Irving T. Diamond, June 9, 1993

**ABSTRACT** Photoreceptors of transgenic mice expressing a mutant rhodopsin gene (Pro<sup>347</sup> → Ser) slowly degenerate. The mechanism of degeneration was studied by aggregation of embryos of normal and transgenic mice to form chimeras. In these chimeras, mosaicism was observed in the coat color, retinal pigment epithelium, and retina. In the retina, the genotype of adjacent patches of normal and transgenic photoreceptors was determined by *in situ* hybridization with a transgene-specific RNA probe. Photoreceptors in the chimeric retina degenerated uniformly, independent of the genotype and similar to the photoreceptors in transgenic mice. However, the chimeric retinas showed varying proportions of normal and transgenic cells. The chimeric retina with a nearly even proportion of normal and transgenic photoreceptors displayed uniform but slower degeneration than that observed in a transgenic mouse of the same age. Our results demonstrate non-autonomy of gene action for the mutated rhodopsin gene and imply that cellular interactions between photoreceptors in the retina probably play a role in degeneration.

Retinitis pigmentosa (RP) describes a heterogeneous group of inherited disorders characterized by progressive dysfunction of photoreceptors. Night blindness typifies early stages of disease, representing reduced rod photoreceptor function. As the disease progresses, impairment of both rod and cone photoreceptor function occurs with subsequent severe loss of visual fields, reflecting widespread degeneration of photoreceptors (1). Autosomal dominant, autosomal recessive, and X chromosome-linked modes of transmission of RP have been described (2). Specifically, >30 mutations in the rhodopsin gene have been identified and shown to correlate with autosomal dominant RP (3–6).

Mechanisms that relate the genetic defect to the phenotype of photoreceptor degeneration remain unknown. Rhodopsin is a glycoprotein produced only by rod photoreceptors. In patients who have mutations in the rhodopsin gene, cone photoreceptors degenerate along with rod photoreceptors although they do not contain any rhodopsin (1). Therefore, we hypothesized that cellular interaction between photoreceptors may have a role in degeneration.

Different laboratories have produced transgenic mouse lines expressing mutant rhodopsin (7–9). In our laboratory, we produced transgenic mice expressing normal or mutant pig rhodopsin (transgene). Transgenic mice which expressed normal pig rhodopsin at levels comparable to endogenous mouse rhodopsin had normal retinas. Those expressing mutant pig rhodopsin at similar levels showed retinal degeneration. We characterized one such transgenic mouse line (Serine 6) expressing a Pro<sup>347</sup> → Ser mutation in the transgene (8). In these mice, retinas developed normally but degener-

ation became noticeable at 3 weeks of age. By 7 weeks, ≈50% of the photoreceptors had degenerated. The process then slowed and was virtually complete by 12 months.

Chimeric mice have been used previously for studying other retinal degeneration mutants, such as the *rd* and *rdS* mice (10–12). The chimeric retinas have a patchy distribution of normal and transgenic rod photoreceptors adjacent to one another, allowing us to study the role of cellular interaction in photoreceptor degeneration.

### MATERIALS AND METHODS

**Construction and Identification of Chimeric Mice.** Chimeras were constructed by embryo aggregation of transgenic and normal mouse lines (13). The two strains employed, a transgenic mouse line hemizygous for a Pro<sup>347</sup> → Ser mutation in the pig rhodopsin gene and a normal strain, shared the same genetic background, C57BL/6. The transgenic strain was constructed by using C57BL/6 mice and maintained by crossing hemizygous individuals with C57BL/6 mice. Potentially transgenic embryos were generated by mating hemizygous transgenic male mice to C57BL/6 female mice. As a result, half of the embryos should be transgenic. The normal mice, C57BL/6J - c<sup>2J</sup>/c<sup>2J</sup> (The Jackson Laboratory), were homozygous for albino, allowing identification of chimeras by coat color mosaicism and by observation of mosaic fundi with indirect ophthalmoscopy. Chimeras expressing the transgene were identified by standard tail-DNA analysis.

**Histology.** Three chimeras expressing the transgene were sacrificed at 7 weeks of age, and the one lacking the transgene, at 14 weeks. Eucleated eyes were immersed in 0.1 M cacodylate buffer, pH 7.3/3% glutaraldehyde. Following overnight fixation at 4°C, eyes were bisected through the optic nerve head along either a superior–inferior or nasal–temporal axis. The eyes were postfixed in 2% osmium tetroxide and embedded in low-viscosity Spurr resin (14). Sections included the entire hemisphere that passed near the optic nerve head. Sections 0.5–1 μm thick were taken and counterstained with toluidine blue dye.

**Construction and Synthesis of Probes for *in Situ* Hybridization.** Two RNA probes were used for *in situ* hybridization; one specific for mouse rhodopsin and the other, pig rhodopsin. These probes were derived from DNA sequences in the 3' untranslated portions of the respective rhodopsin genes. The DNA fragments were cloned in the Novagen T-vector pT7Blue(U) (15). Template for probe synthesis was prepared by linearizing the mouse and pig DNA clones. Radioactive probe was then generated by *in vitro* transcription (15). Plasmid DNA was removed by digestion with RNase-free DNase I (0.1 unit/μl) for 30 min at 37°C.

**In Situ Hybridization.** One eye from one of the chimeras expressing the transgene was analyzed by *in situ* hybridization techniques (15–17). Tissues were exposed for 26 days and, after development, counterstained with hematoxylin and eosin.

**Measurement of Degree of Degeneration of Photoreceptors.** Patches of normal and transgenic photoreceptors were identified by *in situ* hybridization in one chimera expressing the transgene. Sections were analyzed with OPTIMAS 4.0 software (Bioscan, Edmonds, WA) and a microscope equipped with a video camera to measure the height of the photoreceptor outer nuclear layer (ONL). In each section of retina analyzed, a series of heights of the ONL was measured at 4 or 5 cell-length increments along individual patches into bordering genetically different photoreceptor patches. The maximum and minimum heights of a particular patch were noted. The largest variation within a patch was designated as the difference between the two heights. The patches were also studied in relation to flanking photoreceptors of different genotype by comparing the maximum and minimum heights within an individual patch to the corresponding heights of bordering areas. The data were analyzed in this manner to account for variations in specimen sectioning and natural variations of photoreceptor ONL height in different areas of the retina.

**Measurement of Degree of Mosaicism.** We assessed the amount of mosaicism in the chimeras expressing the transgene by quantitating the degree of pigmentation of the retinal pigment epithelium (RPE). In each mouse, we totaled the length of stretches of pigmented and nonpigmented epithelium by using the microscope system and OPTIMAS 4.0 software described above. We used the percentage of nonpigmented cells in the epithelium as an approximation for the percentage of normal cells in the retina. We also directly measured the degree of mosaicism in the chimera analyzed by *in situ* hybridization to validate the use of RPE as an indirect indicator of photoreceptor mosaicism. By this method, photoreceptors delineated by silver grains were distinguished from unmarked photoreceptors.

## RESULTS

**Production of Chimeric Mice.** Four chimeras were identified by coat color mosaicism. Their fundi also demonstrated the presence of pigmented and albino cells (Fig. 1). Of all the mice examined, mosaic fundi were observed only in mice showing coat color mosaicism. The converse was also observed. Furthermore, the extent of mosaicism as judged visually by coat color and fundus examination correlated well

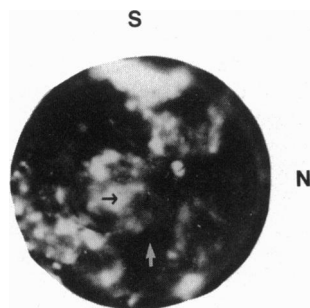


FIG. 1. Fundus of chimera. Normal (black arrow) and transgenic (white arrow) cells are observed. The micrograph focuses on the inferior temporal region, so that several patches of normal cells are poorly delineated in the nasal region of the eye. The proportion of normal and transgenic cells in the retina, as determined visually, corresponds to the measured extent of mosaicism of the chimera. S, superior; N, nasal. ( $\times 16$ .)

for each chimera. Three of the four chimeras expressed the transgene according to analysis of tail DNA.

**Retinal Genotype and Phenotype.** We employed *in situ* hybridization with a pig rhodopsin-specific probe to identify transgenic photoreceptors in the chimeric retina. As a control, we used a mouse rhodopsin-specific probe to identify endogenous mouse rhodopsin mRNA. Hemizygous for the Pro<sup>347</sup>  $\rightarrow$  Ser mutation, transgenic photoreceptors express pig as well as endogenous mouse rhodopsin mRNA. Silver grains were present along the entire length of the retina when the mouse rhodopsin-specific probe was used (Fig. 2A). The highest density of silver grains occurred in the inner segment layer at the junction with the photoreceptor ONL (18–20). With the pig rhodopsin-specific probe, silver grains identified only those cells expressing pig rhodopsin (transgenic photoreceptors). The discontinuity of silver grains along the retina indicated photoreceptors of different genotypes adjacent to one another (Fig. 2B). The patches were more readily delineated in the ONL due to the decreased density of silver grains. In comparison, a leakage effect of the highly dense signal at the level of the inner segments into areas of normal photoreceptors was observed. These extraneous silver grains were probably artifacts and did not signify the presence of pig rhodopsin in areas of normal photoreceptors. Therefore, as shown in Fig. 2B, *in situ* hybridization permitted us to distinguish the two photoreceptor genotypes.

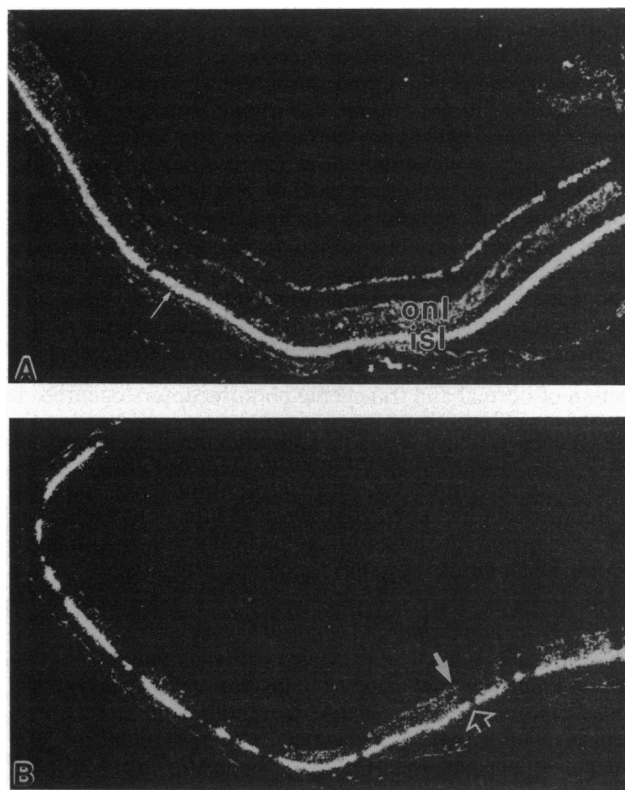


FIG. 2. Dark-field microscopy of chimeric mouse retina, showing *in situ* hybridization. (A) Mouse rhodopsin-specific probe. Silver grains are present along the entire length of the retina. Arrow indicates the area of highest signal density, the inner segment layer at the junction with the ONL. (B) Pig rhodopsin-specific probe. Discontinuity of silver grains along the retina indicates patches of photoreceptors of different genotypes. Solid arrow marks the outer border of one transgenic photoreceptor patch. Decreased density of the silver grains in the ONL enables clear delineation of individual patches. In comparison, the highly dense signal at the inner segment layer demonstrates leakage into areas of normal photoreceptors (open arrow). isl, Inner segment layer. ( $\times 78$ .)

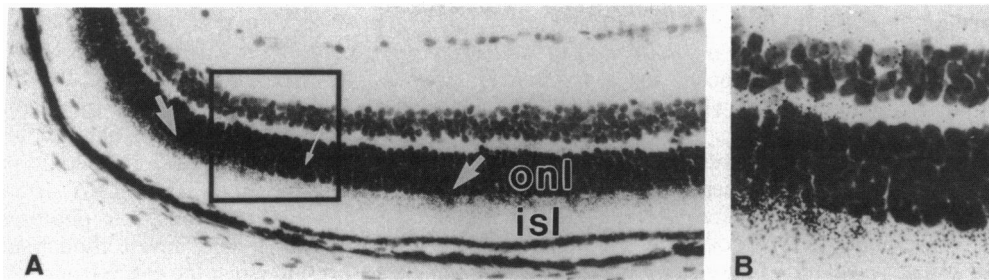


FIG. 3. Bright-field microscopy of chimeric mouse retina, showing *in situ* hybridization with pig rhodopsin-specific probe. Uniform degeneration occurs independently of the genotype of photoreceptors. (A) The thin arrow indicates a patch of normal photoreceptors identified by the near absence of silver grains spanning  $\approx 30$  cells lying between two patches of transgenic photoreceptors characterized by dense signal (thick arrows). ONL shows 7–8 rows of nuclei, whereas 10–11 rows of photoreceptor nuclei are present in the normal retina. ( $\times 250$ .) (B) Magnification of the border region along genetically different patches of photoreceptors as demonstrated by *in situ* hybridization reveals no variation in extent of degeneration. isl, Inner segment layer. ( $\times 400$ .)

Uniform degeneration of photoreceptors in the chimeric retina occurred independently of their genotype. The absence of silver grains characterized normal photoreceptors. In certain patches, signal slightly above background was probably due to the presence of individual transgenic photoreceptors interspersed among the more abundant normal photoreceptors. However, the sparse signal greatly contrasted with the heavy, dense layer of silver grains delineating the transgenic photoreceptors. As an example of the sections analyzed, a patch of normal photoreceptors spanning  $\approx 30$  cells between two patches of transgenic photoreceptors is shown in Fig. 3A. Fig. 3B represents the border region between the adjacent transgenic and normal photoreceptor patches. The ONL shows only 7–8 rows of nuclei, compared with the normal 10–11 appropriate for this region of the retina. Typical of all the patches analyzed, no variation in the extent of degeneration was observed (Fig. 3A and B). Although slight variations ranging from 1 to 2 rows of photoreceptor nuclei did occur within some patches, variations did not demonstrate consistent patterns and did not differ from those seen in the normal mouse. We attributed these differences to natural variations in the retina. Table 1 summarizes the analysis of 157 patches of normal and transgenic photoreceptors in the chimera identified by *in situ* hybridization. The results demonstrated that uniform degeneration of normal and transgenic photoreceptors occurred in the chimeric retina.

Uniform degeneration of the photoreceptors was observed in two other chimeras which expressed the transgene. Fig. 4A and B represent retinal sections from different eyes of one chimera each cut along a separate axis. Fig. 4C is a section from another chimera. The sections shown are from the posterior part of the eye, near the optic nerve head. The ONL shows only 5–6 rows of nuclei, compared with the normal 10–11 for this region of the retina (Fig. 4D).

In the chimera that lacked the transgene, no degeneration occurred. Ten or 11 rows of photoreceptor nuclei in the ONL were present, similar to the normal mouse retina (Fig. 4D).

**Comparison of the Three Chimeras Expressing the Pro<sup>347</sup>  $\rightarrow$  Ser Transgene.** A ratio comparing the amount of nonpigmented and pigmented regions in the RPE was used to indirectly determine the degree of mosaicism of the photoreceptors of each chimera (Table 2). Two of the three chimeras had a small proportion of normal cells, 7% and 16%, respectively. In contrast, the third chimera had 42% normal cells. These percentages were consistent with visual appraisal of the patchy fundi. On direct measurement of the ratio of normal and transgenic photoreceptors in the third chimera by *in situ* hybridization, approximately the same percentage was obtained, supporting the use of RPE as an indirect indicator of photoreceptor mosaicism. Accordingly, we inferred that patches of normal and transgenic photoreceptors existed in similar proportions as the RPE in the first two chimeras.

Uniform degeneration of the photoreceptors was observed in each of the three chimeras. However, the chimeras demonstrated varying degrees of degeneration which correlated with the degree of mosaicism. Degeneration of the photoreceptors in the two chimeras, which were predominantly pigmented and therefore transgenic, resembled that seen in transgenic mice of the same age. On average, five to six rows of photoreceptor nuclei remained at 7 weeks of age; sections shown in Fig. 4A–C are indistinguishable from those of transgenic mice of the same age. In contrast, in the third chimera, which had a more balanced proportion of normal and transgenic photoreceptors, seven to nine rows of photoreceptor nuclei remained at 7 weeks of age (Fig. 4E and F). The height of the ONL was intermediate between that for the retinas of the normal mouse (Fig. 4D) and those of the predominantly transgenic chimeras (Fig. 4A–C). The extent of degeneration resembled that typically observed in a 5-week-old but never a 7-week-old transgenic mouse. These results demonstrated that although degeneration was uniform, the presence of the normal photoreceptors may have retarded degeneration.

Table 1. Variation of degeneration in individual and bordering photoreceptor patches

Photoreceptor genotype	Largest variation within individual patch, $\mu\text{m}$	Difference of maximum height and corresponding height of either adjacent patch, $\mu\text{m}$		Difference of minimum height and corresponding height of either adjacent patch, $\mu\text{m}$	
		R	L	R	L
Transgenic (62 patches)	$0.26 \pm 0.19$	$0.19 \pm 0.17$	$0.18 \pm 0.23$	$0.15 \pm 0.13$	$0.20 \pm 0.20$
Normal (95 patches)	$0.22 \pm 0.19$	$0.15 \pm 0.14$	$0.16 \pm 0.14$	$0.14 \pm 0.17$	$0.14 \pm 0.15$

The degree of variation of degeneration of adjacent areas of photoreceptors and within individual patches of photoreceptors ranged from only one to two rows of photoreceptor nuclei. R, right border; L, left border. One photoreceptor nucleus diameter  $\approx 0.3 \mu\text{m}$ .

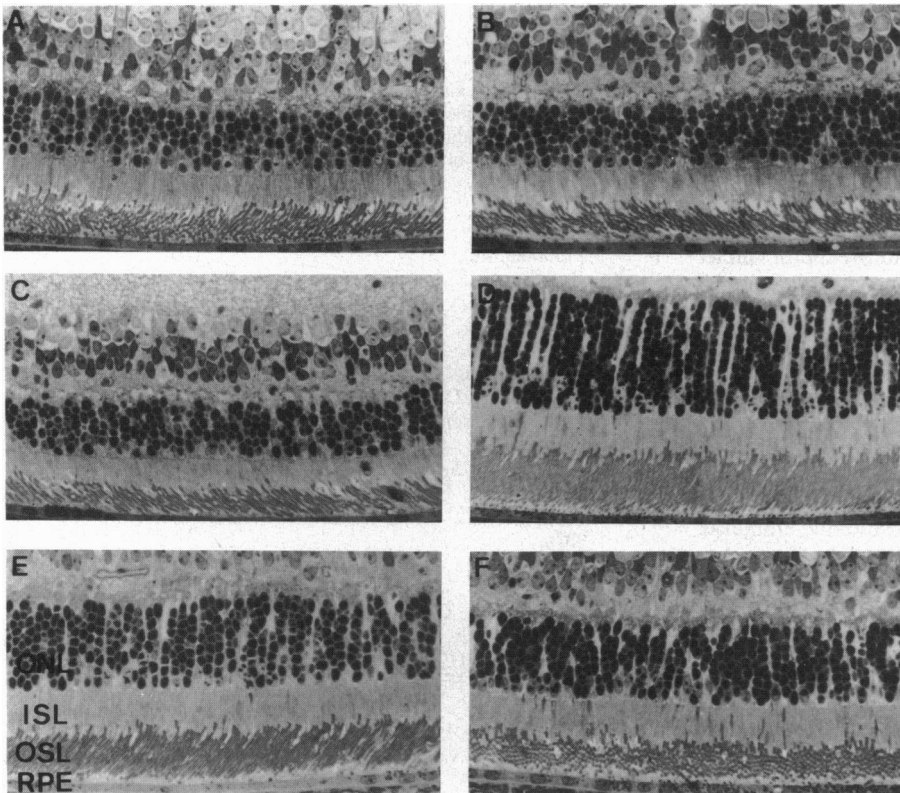


FIG. 4. Histological sections of chimeras expressing the Pro<sup>347</sup> → Ser transgene and a normal mouse. (A) Chimera 1, retina bisected along superior–inferior axis overlying nonpigmented RPE. (B) Chimera 1, retina bisected along nasal–temporal axis overlying nonpigmented RPE. (C) Chimera 2, retina bisected along superior–inferior axis overlying nonpigmented RPE. (D) Normal mouse. Uniform degeneration similar to that of a transgenic mouse is observed in these predominantly transgenic chimeras (A–C). Five to six rows of photoreceptor nuclei are present compared to the 10 or 11 rows observed in a normal mouse (D). (E) Chimera 3, retina overlying nonpigmented RPE. (F) Chimera 3, retina overlying pigmented RPE. Seven to nine rows of photoreceptor nuclei remain (E and F). Height of the ONL is intermediate between that of a normal mouse and that of the predominantly transgenic chimeras (A–C). Uniform degeneration, independent of RPE genotype, is observed in all three chimeras. ISL, inner segment layer; OSL, outer segment layer. (Toluidine blue; ×400.)

**RPE Genotype and Retinal Phenotype.** Consistent with results from earlier work (10–12), both pigmented and nonpigmented cells were observed in the RPE of the chimeras. In none of the mice was the RPE completely one phenotype. The RPE of two of the four chimeras was predominantly pigmented, whereas the proportion of pigmented and nonpigmented cells was more balanced in the remaining two chimeras. In each of the three chimeras expressing the transgene, the photoreceptor ONL was studied in relation to RPE genotype. Fig. 4 A–C represent retinal sections of two of the chimeras overlying nonpigmented RPE. Fig. 4 E and F depict retinal sections of the remaining chimera expressing the transgene overlying nonpigmented and pigmented RPE, respectively. Uniform degeneration of the photoreceptors was observed under large stretches of nonpigmented as well as pigmented RPE. Since the rhodopsin gene is specific to the rod photoreceptors, we did not anticipate that the mechanism of photoreceptor degeneration and cell death due to the Pro<sup>347</sup> → Ser mutation would act primarily through the RPE.

## DISCUSSION

**Implications for Pathogenesis of Photoreceptor Degeneration.** Uniform degeneration of photoreceptors in the chimeric retina, independent of genotype, implicates cellular interaction between normal and transgenic cells in the mechanism leading to degeneration caused by the Pro<sup>347</sup> → Ser mutation

in the rhodopsin gene. Patchy degeneration was not observed, as would be expected if the photoreceptors derived from the normal embryo did not degenerate. Areas of normal photoreceptors would be anticipated if the mechanism leading to degeneration was completely cell-autonomous. Therefore, both the genetic mutation and cellular interaction play a role in photoreceptor death caused by mutations in the rhodopsin gene.

Although the data implicate a role for cellular interaction, they do not pinpoint the mechanism leading to photoreceptor degeneration. One theory suggests that transgenic photoreceptors produce a toxic factor that disrupts the retinal environment and causes death of neighboring photoreceptors. The data do not support such a theory. Uniform degeneration was observed in large patches of normal rod photoreceptors. In the presence of a diffusible toxic factor, normal rod photoreceptors lying adjacent to transgenic photoreceptors, and therefore the toxin, would be expected to degenerate to a greater extent than those farther away. Analysis of large patches of normal photoreceptors (up to 50 cells in length) revealed no appreciable variation in the degree of degeneration within individual patches. More importantly, the idea of a toxic factor does not explain the apparent remedial effects of the presence of normal photoreceptors. In a chimera which had 42% normal cells in the retina, the photoreceptors did not degenerate to the degree seen in the transgenic mice. Another theory argues that remaining nor-

Table 2. Degree of mosaicism of three chimeras carrying the Pro<sup>347</sup> → Ser transgene

Mouse	Method of measurement	Total length, $\mu\text{m}$			Normal cells, %
		Cells derived from transgenic embryo	Cells derived from normal embryo	Retina	
1 (9 sections)	RPE (indirect)	2531.7	189.7	2721.4	6.9
2 (9 sections)	RPE (indirect)	2171.7	422.0	2593.7	16.3
3 (7 sections)	RPE (indirect)	1521.4	1117.9	2639.3	42.4
3 (7 sections)	<i>In situ</i> (direct)	988.7	714.7	1703.4	42.0

In one chimera, direct measurement of the ratio of normal and transgenic photoreceptors by *in situ* hybridization supports the use of RPE as an indirect indicator of photoreceptor mosaicism.

mal photoreceptors migrate to fill vacant spaces as transgenic photoreceptors degenerate. However, the patchy distribution of the two types of photoreceptors and the uniformity of the ONL in the degenerating chimeric retina argue against such an explanation.

Conclusions derived from this study differ from those of previous work on chimeras expressing the *rd* and *rds* retinal degeneration mutations (10–12). Mutant photoreceptors died on schedule while normal photoreceptors did not degenerate. Areas of the retina with 8–10 rows of photoreceptor nuclei were observed adjacent to areas with 1–4 rows of photoreceptor nuclei (10–12). In contrast, in the present study, uniform degeneration occurred and the chimera with an approximately even proportion of normal cells displayed retarded degeneration. It is now known that the *rd* mutation is due to a defect in the  $\beta$  subunit of cGMP phosphodiesterase gene (20, 21) and that the *rds* mutation is due to a defect in the peripherin/*rds* gene (22, 23). Like mutations in the rhodopsin gene, those in the human analogs of the *rd* (24) and *rds* (6) genes also cause RP. Results from studying chimeras suggest that different mechanisms may lead to photoreceptor degeneration.

A theory that involves a trophic factor, a substance necessary for photoreceptor survival, might explain our findings. We may assume that each photoreceptor releases this trophic factor but also takes it up for survival. Normally, each photoreceptor contributes to and draws from a common pool of this factor in the retina. Suppose that some photoreceptors—namely, those that are transgenic—contribute less than the normal amount to the pool but continue to consume the same quantity of this factor: the supply diminishes, becoming insufficient for both normal and transgenic photoreceptors. Eventually, this leads to death of both types of photoreceptors.

This theory is attractive because it explains the observed nonautonomy of gene action—both normal and transgenic photoreceptors in the chimeric retina are subject to the same hazard. Further, it accounts for the dependence on the proportion of normal photoreceptors in the degeneration of the chimeric retina. In the presence of more normal photoreceptors and concomitantly fewer mutant photoreceptors, this trophic factor is present in the retina at a concentration nearer normal levels, resulting in longer survival of the photoreceptors. Therefore, degeneration of both types of photoreceptors would occur at a slower rate. In contrast, in the presence of more mutant photoreceptors, decreased contribution to the supply of this trophic factor would accelerate photoreceptor degeneration.

Recent studies (25) have revealed that growth factors, cytokines, and neurotrophins may delay degeneration of light-damaged photoreceptors, although the mechanism of rescue remains unknown. The theory described above may provide a framework to explore further the mechanisms through which rescuing agents act. The theory also has implications for the mechanisms of pathogenesis in patients

with autosomal dominant RP caused by mutations in the rhodopsin gene.

This study was supported in part by National Institutes of Health Grants RO1 EY06862 and R55 EY09047 and a grant from the Retinitis Pigmentosa Foundation (to F.W.) and by Grant RO1 EY09738 (to R.M.P.). P.C.H. is a Howard Hughes Medical Institute research fellow.

1. Heckenlively, J. R. (1988) *Retinitis Pigmentosa* (Lippincott, Philadelphia).
2. Boughman, J. A. & Fishman, G. A. (1983) *Br. J. Ophthalmol.* **67**, 449–454.
3. Dryja, T. P., McGee, T. L., Hahn, L. B., Cowley, G. S., Olsson, J. E., Reichel, E., Sandberg, M. A. & Berson, E. L. (1990) *N. Engl. J. Med.* **323**, 1302–1307.
4. Sung, C. H., Davenport, C. M., Hennessey, J. C., Maumenee, I. H., Jacobsen, S. G., Heckenlively, J. R., Nowakowski, R., Fishman, G., Gouras, P. & Nathans, J. (1991) *Proc. Natl. Acad. Sci. USA* **88**, 6481–6485.
5. Dryja, T. P., Hahn, L. B., Cowley, G. S., McGee, T. L. & Berson, E. L. (1991) *Proc. Natl. Acad. Sci. USA* **88**, 9370–9374.
6. Berson, E. L. (1993) *Invest. Ophthalmol. Vis. Sci.* **34**, 1659–1676.
7. Olsson, J. E., Gordon, J. W., Pawlyk, B. S., Roof, D., Hayes, A., Molday, R. S., Mukai, S., Cowley, G. S., Berson, E. L. & Dryja, T. P. (1992) *Neuron* **9**, 815–830.
8. Wong, F. & Hao, Y. (1992) *Invest. Ophthalmol. Vis. Sci.* **33**, 944 (abstr.).
9. Naash, M. I., Hollyfield, J. G., Al-Ubaidi, M. R. & Baehr, W. (1993) *Proc. Natl. Acad. Sci. USA* **90**, 5499–5503.
10. LaVail, M. M. & Mullen, R. J. (1976) *Exp. Eye Res.* **23**, 227–245.
11. Sanyal, S. & Zeilmaker, G. H. (1984) *Exp. Eye Res.* **39**, 231–245.
12. Sanyal, S., Hawkins, R. K. & Zeilmaker, G. H. (1988) *Curr. Eye Res.* **7**, 1183–1190.
13. Petters, R. M. & Mettus, R. V. (1984) *Theriogenology* **22**, 167–174.
14. Spurr, A. R. (1969) *J. Ultrastruct.* **26**, 31–42.
15. Novagen (1991) *Suresite In Situ Hybridization Manual* (Novagen, Madison, WI).
16. Blumberg, D. D. (1987) *Methods Enzymol.* **152**, 20–24.
17. Larsson, L. I. (1989) *Histochem. J.* **21**, 435–440.
18. Brann, M. R. & Young, W. S. (1986) *FEBS Lett.* **200**, 275–278.
19. Treisman, J. E., Morabito, M. A. & Barnstable, C. (1988) *Mol. Cell. Biol.* **8**, 1570–1579.
20. Bowes, C., Li, T., Danciger, M., Baxter, L. C., Applebury, M. L. & Farber, D. B. (1990) *Nature (London)* **347**, 677–680.
21. Pittler, S. J. & Baehr, W. (1991) *Proc. Natl. Acad. Sci. USA* **88**, 8322–8326.
22. Travis, G. H., Sutcliffe, J. G. & Bok, D. (1991) *Neuron* **6**, 61–70.
23. Connell, G., Boscom, R., Molday, L., Reid, D., McInnes, R. R. & Molday, R. S. (1991) *Proc. Natl. Acad. Sci. USA* **88**, 723–726.
24. McLaughlin, M. E., Sandberg, M. A., Berson, E. L. & Dryja, T. P. (1993) *Nat. Genet.* **4**, 130–134.
25. LaVail, M. M., Unoki, K., Yasumura, D., Matthes, M. T., Yancopoulos, G. D. & Steinberg, R. H. (1992) *Proc. Natl. Acad. Sci. USA* **89**, 11249–11253.